Finite Asymmetric Deformation of Shallow Spherical Shells

J. FAMILI* AND R. R. ARCHER†
Case Institute of Technology, Cleveland, Ohio

A procedure is developed for the integration of the system of nonlinear partial differential equations governing the asymmetric deformation of shallow spherical shells. A suitable iteration scheme based on a finite-difference approach is shown to yield the asymmetric postbuckling states for the spherical cap under uniform pressure. Thus, the practically important asymmetric "lower buckling load" is systematically computed for the first time. Applications to more general asymmetric buckling problems are indicated by the example of the half-loaded spherical cap.

1. Introduction

OVER the past ten years considerable effort has gone into the integration of the equations for the finite deformation of shallow spherical shells. The first phase of the work was concerned with the development of analytic techniques for the accurate mathematical description of the finite axisymmetric deformation of shallow spherical shells.[1–4] The pace of the research was determined in no small degree by the increasing power and availability of high-speed computing devices.

The second phase began with the work of Weinitschke[5] and Huang[6] in which the problem of the clamped spherical cap under uniform pressure was studied to find out if asymmetric buckling of the classical bifurcation type could take place for certain ranges of shell geometries before the symmetric snap-through occurred. Thus the restriction to axisymmetric deformations, which had been imposed in previous work, was relaxed only to the extent that small asymmetric deformations in the neighborhood of the "primary" symmetric deformation state were allowed. In both Refs. 5 and 6 it was found that the asymmetric bifurcation buckling loads were less than the symmetric snap-through loads over a wide range of shell geometries, as shown in Fig. 1. However, the results of Refs. 5 and 6 were in serious disagreement as is evident from Fig. 1. In Ref. 7, very close agreement with the loads computed by Huang resulted when the problem was studied within the context of the small asymmetric vibration of the shell in the neighborhood of the symmetric primary state. Also, recent, very carefully conducted experiments by Krenzke and Kiernan[8] on the buckling of spherical caps indicate (Fig. 1) a far better correlation between theory and experiment than was previously found, provided the minimum of either the symmetric snap-through load or the asymmetric bifurcation load is chosen for the buckling load.

In the light of progress that has been achieved, it would seem that the next phase of work should be concerned with the difficult area of finite asymmetric deformations of shells. This work is necessary both in order to achieve further understanding of the snap-buckling problem by studying the asymmetric postbuckling behavior of a shallow cap as well as to broaden the scope of problems for which stability predictions can be made to include nonsymmetrically loaded and supported shells.

It is our objective in this paper to develop a suitably general method for the integration of the nonlinear partial differential equations governing the finite deformations of shallow shells so that problems of the type just described can be effectively handled.

2. Basic Equations

Consider the class of problems governed by Marguerre's equations[9] expressed in terms of the tangential, circumferential, and normal deflections u, v, and w and written using polar coordinates in the form,‡

$$u'' + \frac{u'}{r} - \frac{u}{r^2} + \left(\frac{1-\nu}{2}\right)\frac{u^{\cdot\cdot}}{r^2} + \left(\frac{1+\nu}{2}\right)\frac{v^{\cdot\prime}}{r} - \left(\frac{3-\nu}{2}\right)\frac{v^{\cdot}}{r^2} + w'\left[-z'' - \frac{\nu z'}{r} + w'' + \left(\frac{1-\nu}{2}\right)\left(\frac{w'}{r} + \frac{w^{\cdot\cdot}}{r^2}\right)\right] + \left(\frac{1+\nu}{2}\right)\frac{w^{\cdot}}{r}\left(\frac{w^{\cdot}}{r}\right)' + w\left(-z''' + \frac{z'}{r^2} - \frac{z''}{r}\right) = 0 \quad (1)$$

$$\left(\frac{1-\nu}{2}\right)\left(v'' + \frac{v'}{r} - \frac{v}{r^2}\right) + \frac{v^{\cdot\cdot}}{r^2} + \left(\frac{1+\nu}{2}\right)\frac{u^{\prime\cdot}}{r} + \left(\frac{3-\nu}{2}\right)\frac{u^{\cdot}}{r^2} + w'\left[\left(\frac{1+\nu}{2}\right)\frac{w^{\prime\cdot}}{r} + \left(\frac{1-\nu}{2}\right)\frac{w^{\cdot}}{r^2}\right] + w^{\cdot}\left[\frac{-z'}{r^2} - \frac{\nu z''}{r} + \frac{1-\nu}{2}\frac{w''}{r} + \frac{w^{\cdot\cdot}}{r^3}\right] = 0 \quad (2)$$

$$-D\nabla^4 w + N_r(z'' + w'') + N_\theta\left(\frac{z' + w'}{r} + \frac{w^{\cdot\cdot}}{r^2}\right) + 2N_{r\theta}\left(\frac{w^{\cdot}}{r}\right)' = -q \quad (3)$$

$$N_r = [Eh/(1-\nu^2)](\epsilon_r + \nu\epsilon_\theta) \quad (4a)$$

$$N_\theta = [Eh/(1-\nu^2)](\epsilon_\theta + \nu\epsilon_r) \quad (4b)$$

$$N_{r\theta} = [Eh/2(1+\nu)]\gamma_{r\theta} \quad (4c)$$

$$\epsilon_r = u' - z''w + \tfrac{1}{2}w'^2 \quad (4d)$$

$$\epsilon_\theta = u/r + v^{\cdot}/r - (z'/r)w + \tfrac{1}{2}w^{\cdot 2}/r^2 \quad (4e)$$

$$\gamma_{r\theta} = u^{\cdot}/r + v' - v/r + w'w^{\cdot}/r \quad (4f)$$

and where N_r, N_θ, and $N_{r\theta}$ are membrane stress resultants, ϵ_r, ϵ_θ, $\gamma_{r\theta}$ the membrane strains, r the radial coordinate, $z(r)$ the representation of the initial middle surface (defined in

Received June 12, 1964; revision received September 28, 1964. The work of both authors was supported in part by a National Science Foundation Grant (GP-938) to the Case Institute of Technology. The authors would also like to express their appreciation to the Andrew R. Jennings Computing Center at Case, which is supported in part by a National Science Foundation Grant, for making computation time available for this work.

* Research Assistant.

† Associate Professor.

‡ We have included only the z terms corresponding to shells of revolution, although the addition of the $z^{\cdot}$ and $z^{\cdot\cdot}$ terms for more general shells is possible here.

accordance with Fig. 2), E, ν the material constants, h the thickness of the shell, $D = Eh^3/12(1 - \nu^2)$ the bending stiffness, and $q(r, \theta)$ the normal loading.

Also

$$( )' = (\partial/\partial r)( ) \qquad ( )^{\cdot} = (\partial/\partial\theta)( ) \tag{5a}$$

$$\nabla^2( ) = ( )'' + ( )'/r + ( )^{\cdot\cdot}/r^2 \tag{5b}$$

Equations (1–3) are given in a form convenient for the analysis of classes of shallow shells with arbitrary loads and middle surface geometry as well as for a variety of support conditions provided that the boundary consists of segments of the polar coordinate lines; otherwise the rectangular coordinate form is perhaps preferable. In what follows we restrict attention to complete initially spherical shells clamped around their entire edge but subjected to arbitrary loads $g(r, \theta)$.

A convenient nondimensional form follows if we write

$$z = (a^2 - r^2)/2R \qquad x = r/a \tag{5c}$$

$$m^4 = 12(1 - \nu^2) \qquad q_{CR} = 4Eh^2/R^2m^2 \tag{5d}$$

$$\lambda^2 = m^2a^2/Rh \qquad p(x, \theta) = -q(x, \theta)/q_{CR} \tag{5e}$$

$$( )' = (\partial/\partial x)( ) \qquad \bar{u} = au/h^2 \tag{5f}$$

$$\bar{v} = av/h^2 \qquad \bar{w} = w/h \tag{5g}$$

$$\nabla^2( ) = ( )'' + ( )'/x + ( )^{\cdot\cdot}/x^2 \tag{5h}$$

and get

$$\bar{u}'' + \frac{\bar{u}'}{x} - \frac{\bar{u}}{x^2} + \frac{1 - \nu}{2}\frac{\ddot{\bar{u}}}{x^2} + \frac{1 + \nu}{2}\frac{\dot{\bar{v}}'}{x} - \frac{(3 - \nu)}{2}\frac{\dot{\bar{v}}}{x^2} + (1 + \nu)\frac{\lambda^2}{m^2}\bar{w}' = -\bar{w}'\bar{w}'' - \frac{(1 - \nu)}{2} \times \left(\frac{\bar{w}'^2}{x} + \frac{1}{x^2}\bar{w}'\dot{\bar{w}}\right) - \frac{1 + \nu}{2}\frac{\dot{\bar{w}}}{x}\left(\frac{\dot{\bar{w}}}{x}\right)' \tag{6}$$

$$\frac{1 - \nu}{2}\left(\bar{v}'' + \frac{\bar{v}'}{x} - \frac{\bar{v}}{x^2}\right) + \frac{\ddot{\bar{v}}}{x^2} + \frac{1 + \nu}{2}\frac{\dot{\bar{u}}'}{x} + \frac{(3 - \nu)}{2}\frac{\dot{\bar{u}}}{x^2} + (1 + \nu)\frac{\lambda^2}{m^2}\frac{\dot{\bar{w}}}{x} = -\bar{w}'\left(\frac{1 + \nu}{2}\frac{\dot{\bar{w}}'}{x} + \frac{1 - \nu}{2}\frac{\dot{\bar{w}}}{x^2}\right) - \dot{\bar{w}}\left(\frac{1 - \nu}{2}\frac{\bar{w}''}{x} + \frac{\ddot{\bar{w}}}{x^3}\right) \tag{7}$$

$$\nabla^4\bar{w} + \frac{m^2\lambda^2}{1 - \nu}\left(\bar{u}' + \frac{2\lambda^2}{m^2}\bar{w} + \frac{\bar{u}}{x} + \frac{\dot{\bar{v}}}{x}\right) = -\frac{m^2\lambda^2}{2(1 - \nu)}\left(\bar{w}'^2 + \frac{\dot{\bar{w}}^2}{x^2}\right) + 12\nabla^2\bar{w}\left[\frac{\bar{u}}{x} + \frac{\dot{\bar{v}}}{x} + \frac{\lambda^2}{m^2}\bar{w} + \frac{1}{2}\frac{\dot{\bar{w}}^2}{x^2} + \nu\left(\bar{u}' + \frac{\lambda^2}{m^2}\bar{w} + \frac{1}{2}\bar{w}'^2\right)\right] - 12(1 - \nu)\bar{w}''\left(\frac{\bar{u}}{x} - \bar{u}' + \frac{\dot{\bar{v}}}{x} - \frac{1}{2}\bar{w}'^2 + \frac{1}{2}\frac{\dot{\bar{w}}^2}{x^2}\right) + 12(1 - \nu)\left[\frac{\dot{\bar{u}}}{x} + \bar{v}' - \frac{\bar{v}}{x} + \frac{\bar{w}'\dot{\bar{w}}}{x}\right]\left(\frac{\dot{\bar{w}}'}{x} - \frac{\dot{\bar{w}}}{x^2}\right) - \frac{4\lambda^4}{m^2}p(x, \theta) \tag{8}$$

with the boundary conditions

$$x = 1 \qquad \bar{u} = \bar{v} = \bar{w} = (\partial\bar{w}/\partial x) = 0 \tag{9}$$

3. Method of Solution

An extensive literature describing numerical methods for the solution of elliptic-type linear partial differential equations§ exists but, aside from a few special equations, very little information is available to help in designing methods for the integration of a high-order system of nonlinear equations such as (6–8) represent. Considerable experimentation with various iterative and direct solution techniques leads to agonizingly slow computations even on some of the fastest computers presently available and are hardly suitable for an analysis that requires solutions over a fairly wide range of load values. The basic problem is that, just as for the nonlinear boundary-value problems solved in Refs. 1–4 and the nonlinear eigenvalue problems in Refs. 5–7, it was necessary to have a means for the accurate solution of a sequence of linear boundary-value problems in order to solve the nonlinear problems, so we have the same requirement here except that now our linear boundary-value problems involve partial differential equations. Most of the efficient techniques for solving these boundary-value problems are iterative techniques contrasted with the direct solution techniques that were possible, even for the relatively high-order ordinary differential systems encountered in Refs. 1–7. Most of the devices for accelerating the convergence of iterative methods for the solution of partial differential equations are developed only for linear equations.[10]

In what follows we have attempted to achieve a balance between the rates of convergence associated with the two basic iterations present in the method of solution to the problem represented by Eqs. (6–9).

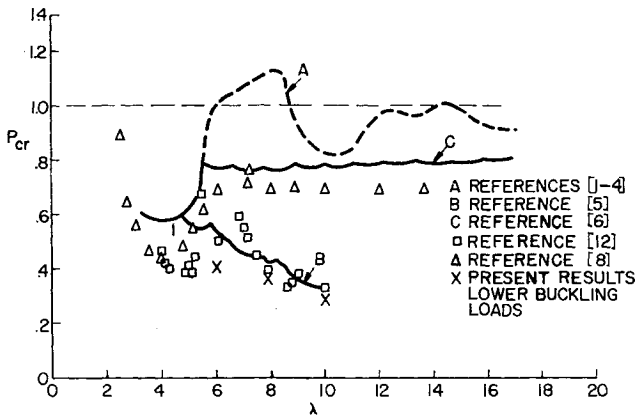

Fig. 1. Summary of theoretical and experimental results for the buckling of a clamped spherical shell. Curve *A* represents theoretical loads based on an axisymmetric theory. Curves *B*, *C*, and the present results are based on an asymmetric theory. The experimental results of Refs. 8 and 12 are shown for comparison.

A. Block Tridiagonal Iterative Scheme

If we introduce the variable

$$\phi = \nabla^2 w \tag{10}$$

then Eqs. (6–9) reduce to a system of four second-order non-

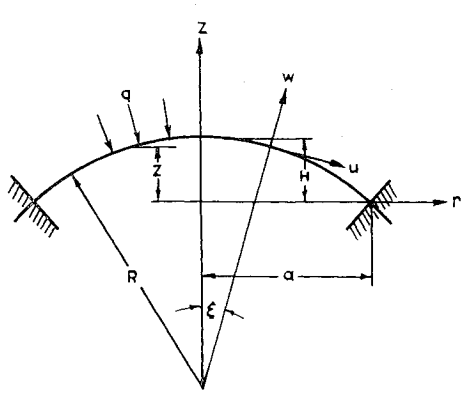

Fig. 2. Geometry of shell.

§ See Ref. 10 for a discussion of iterative techniques for such problems as well as a very complete bibliography.

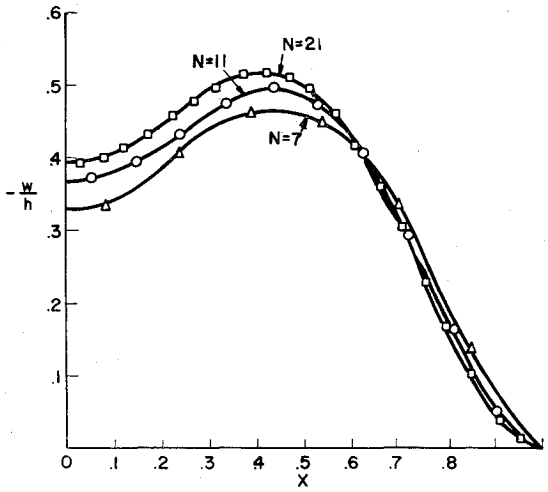

Fig. 3. Comparison of the normal deflection under uniform load computed at a θ = const section using the asymmetric theory with $N=7$, $M=6$ with the more accurate results from the axisymmetric theory in Ref. 4 with $N=11$, 21 for $p=0.7$, which is just below the upper buckling load ($\lambda=6.0$).

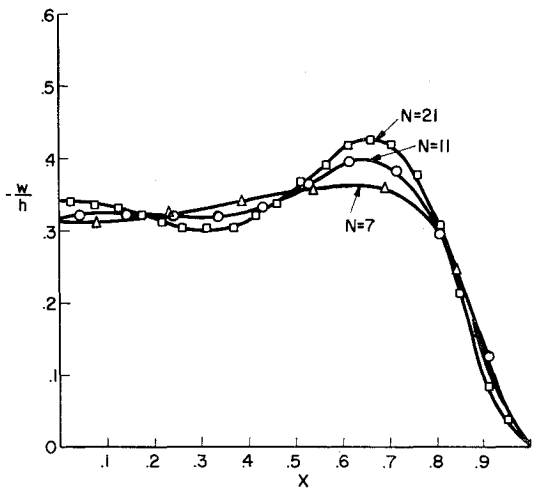

Fig. 4. Comparison of the normal deflection under uniform load computed at a θ = const section using the asymmetric theory with $N=7$, $M=6$ with the more accurate results from the axisymmetric theory in Ref. 4 with $N=11$, 25 for $p=0.7$, which is just below the upper buckling load ($\lambda=10.0$).

linear partial differential equations in terms of the variables u, v, w, ϕ. If we replace all derivatives by simple central difference expressions based on the spacings h_x and h_θ in the x and θ directions, respectively, and if all nonlinear terms are replaced by series expansions about the kth iterate terms in powers of the difference between the $k+1$st and kth iterate¶ and all linear terms are labeled $k+1$st iterate, then retention of only first-order terms in the series expansions will lead to a sequence of systems of linear algebraic equations which approximate the original system of equations (6–10) in the following sense. If, to within a prescribed accuracy, the limiting solution of this sequence of linear systems is found, then this limiting solution has the property that, to within terms of second-order in h_x and h_θ, the differences of this solution approximate the derivatives in the nonlinear equations (6–10).

The numerical problem then reduces to developing an efficient way of solving the linear system of $4(N \times M)$ algebraic equations. These equations have the property that, corresponding to each internal point in the finite-difference network, we can write

$$A_{ij}T_{i-1,\,j} + B_{ij}T_{i,\,j} + C_{ij}T_{i+1,\,j} = D_{ij} + E_{ij}T_{i,\,j+1} + F_{ij}T_{i,\,j-1} \quad (11a)$$

$$i = 1, 2, \ldots, N \qquad j = 1, 2, \ldots, M \quad (11b)$$

where

$$T_{i,\,j} = \begin{pmatrix} u^{k+1} \\ v^{k+1} \\ w^{k+1} \\ \phi^{k+1} \end{pmatrix}_{i,\,j} \quad (11c)$$

and $u_{i,\,j}{}^{k+1}$ $v_{i,\,j}{}^{k+1}$, $w_{i,\,j}{}^{k+1}$, $_i\phi_{,\,j}{}^{k+1}$ are values of the displacement variables at the $k+1$st interation corresponding to point x_i, θ_j. A_{ij}, B_{ij}, C_{ij}, E_{ij}, F_{ij} are 4×4 matrices,** the elements of which involve the quantities ν, x_i, λ, u, v, w, ϕ and the derivatives of u, v, w, ϕ at the kth iteration stage.

The points in the finite-difference network are taken on the concentric circles of radius $h_x/2$, $3h_x/2$, etc.; thus, for points on the smallest circle, Eq. (11) becomes

$$B_{1j}T_{1,\,j} + C_{1j}T_{2,\,j} = \bar{D}_{1j} \quad (12a)$$

where

$$\bar{D}_{1j} = D_{1j} + E_{1j}T_{1,\,j+1} + F_{1j}T_{1,\,j-1} - A_{1j}T_{0,\,j}$$

At station N-1, Eq. (11a) can be written as

$$A_{N-1,\,j}T_{N-2,\,j} + B_{N-1,\,j}T_{N-1,\,j} + C_{N-1,\,j}T_{N,\,j} = D_{N-1,\,j} + E_{N-1,\,j}T_{N-1,\,j+1} + F_{N-1,\,j}T_{N-1,\,j-1} \quad (12b)$$

where

$$T_{N,\,j} = \begin{pmatrix} 0 \\ 0 \\ 0 \\ \phi \end{pmatrix}_{N,\,j}$$

By introducing the point $i = N+1$ in each radial direction outside the edge of the shell, $\phi_{N,\,j}$ can be obtained from Eq. (10) since

$$h_x{}^2\phi_{N,\,j} = w_{N+1,\,j} - 2w_{N,\,j} + w_{N-1,\,j}$$

or

$$\phi_{N,j} = (2/h_x{}^2)w_{N-1,\,j} \quad (12c)$$

Therefore Eq. (12b) can be written as

$$A_{N-1,\,j}T_{N-2,\,j} + B_{N-1,\,j}T_{N-1,\,j} = \bar{D}_{N-1,\,j} \quad (13)$$

where

$$\bar{D}_{N-1,\,j} = D_{N-1,\,j} + E_{N-1,\,j}T_{N-1,\,j+1} + F_{N-1,\,j}T_{N-1,\,j-1} - C_{N-1,\,j}T_{N,\,j}$$

Equations (11–13) represent, for each fixed j, a block tridiagonal system for the N-1 unknowns $T_{1,j}, \ldots, T_{N-1,\,j}$ as long as all $T_{i,j}$ terms on the right sides of Eqs. (11a, 12a, and 13) are assumed known from the previous states of the calculation. As each new radial line of T's are computed, they are introduced both into the A_{ij}, B_{ij}, C_{ij}, and $\bar{D}_{ij}$ as well as the T terms of the right side of Eqs. (11a, 12a, and 13).

4. Computational Techniques

Since for each load step it is necessary to carry out a number of "sweeps" over the entire network in order to achieve a given degree of convergence, and since many load steps are required in order to examine a wide enough range of loading to reveal the pre- and postbuckling behavior of the shell, it is necessary to restrict the number of internal points in order

¶ For example, if f and g are any two functions, then the nonlinear term fg would be replaced by $f^kg^k + f^k(g^{k+1} - g^k) + g^k(f^{k+1} - f^k)$ + higher-order terms.

** The elements of these matrices are given in Ref. 11.

to stay within reasonable computation time limits. In the work reported here, we took $N = 7$ and $M = 6$–8 (this corresponds to 144–192 unknown values for the u, v, w, ϕ). In Fig. 3 and 4 the solutions for w computed with $N = 7$ and $M = 6$ are compared with the more accurate solutions for $N = 11$ and 21 computed from the axisymmetric theory in Ref. 4 for a value of p near the load for which bifurcation from the axisymmetric load is predicted. As expected, the 7-point approximation degenerates as the deflection mode becomes more complicated with increasing λ.

5. Asymmetrical Postbuckling of a Uniformly Loaded Spherical Cap

Since the objective here is the determination of the behavior of the shell after bifurcation from the axisymmetric states has occurred, it would be preferable to start at the known (axisymmetric) state at the bifurcation load and then proceed with the postbuckling analysis. However, it turns out that a more practical approach is to introduce the slightly asymmetric load $p(x, \theta) = p_0(1 + \epsilon \sin\theta)$ and generate the load-deflection curve for this snap-through problem. In Fig. 5 the curve for $\epsilon = 0.05$ is shown. This avoids the mathematical difficulties associated with attempting to achieve the postbuckling states in the neighborhood of the point U (in Fig. 5) where axisymmetric states result from the asymmetric theory when the load is decreased from the value at U. With the "load imperfection" method it is possible, through small load steps, to achieve the asymmetric states over the range corresponding to the section UL of the $\epsilon = 0.0$ curve. Then, by reducing ϵ to zero in small steps, the transition from point A to point C in Fig. 5 can be accomplished. From C it is possible to compute the entire range of the postbuckling curve from the bifurcation load at U to the "lower buckling load" at the point L. In the computation of the $\epsilon = 0.0$ curve, a maximum error of 0.1% was used as a convergence criterion, whereas for $\epsilon = 0.05$ a 1% criterion was used. The approach to U was signaled by a decrease in the circumferential displacements v until they reached a level comparable with those present in the branch $0U$ due to small accumulated errors in the asymmetric solution of the axisymmetric states on $0U$. The u, w, ϕ values compare very well in the neighborhood of U at least to within the accuracy of the calculations. Thus, the bifurcation load p_U lies somewhere between 0.72–0.74. This compares very well with the value of 0.777 computed in Refs. 6 and 7 (using from 36 to 40 points in the radial direction), considering the relatively crude network of points in the radial direction used here.

In Ref. 6 the asymmetric buckling mode for $\lambda = 6$, based on a linearized theory in the neighborhood of the axisymmetric deflection state, was found to have a radial node at the apex and its maximum value approximately half way from the apex to the edge. Also it was proportional to $\cos 2\theta$.

The postbuckling deflection states computed in this paper over the range p_U to p_L were strongly asymmetric. Because of the relatively few mesh points in the solution, it was difficult to identify the radial mode shape discussed previously with any precision; however, there was some indication that it was present. The results for the circumferential mode shape indicated that several harmonics were present including $\cos\theta$ and $\cos 2\theta$.

In Fig. 6 the results for $\lambda = 10.0$ are shown, as well as the more accurately computed axisymmetric curve $N = 21$. As would be anticipated from Fig. 4, the effect of the reduction in the number of radial points is substantial; however, the predicted bifurcation load 0.73–0.75 is to be compared with 0.778 computed in Refs. 6 and 7.

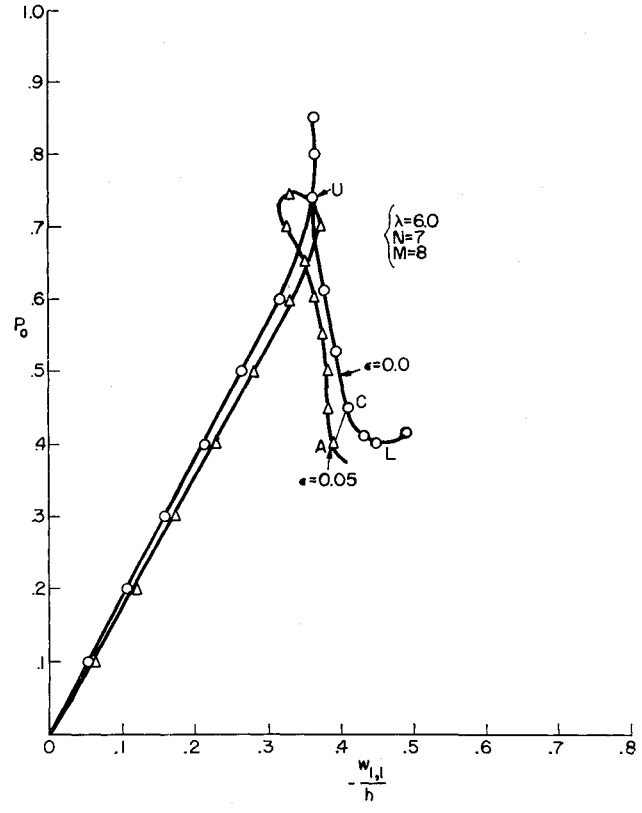

Fig. 5. Load-deflection curves for the loading $p = p_0(1 + \epsilon \sin\theta)$ showing prebuckling and postbuckling ranges for the deflection point $w_{1,1}$ (near the apex of the shell) corresponding to a uniform load ($\epsilon = 0$) and a slightly asymmetric load ($\epsilon = 0.05$).

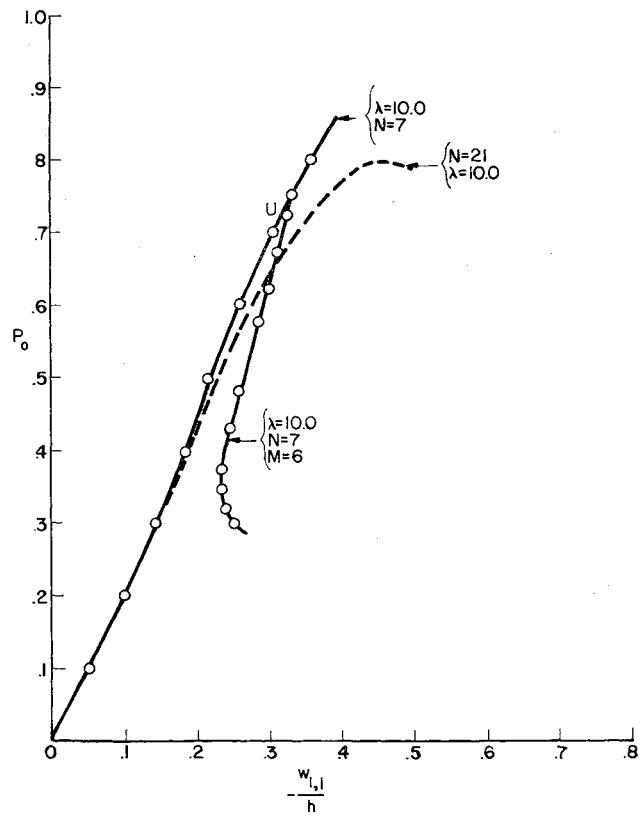

Fig. 6. Load-deflection curves for a uniform load showing prebuckling and postbuckling ranges for the deflection point $w_{1,1}$ (near the apex of the shell) and including the more accurate curve for $N = 21$ computed in Ref. 4 as well as the extension of the load deflection curve beyond the upper buckling load based on the axisymmetric theory in Ref. 4 with $N = 7$.

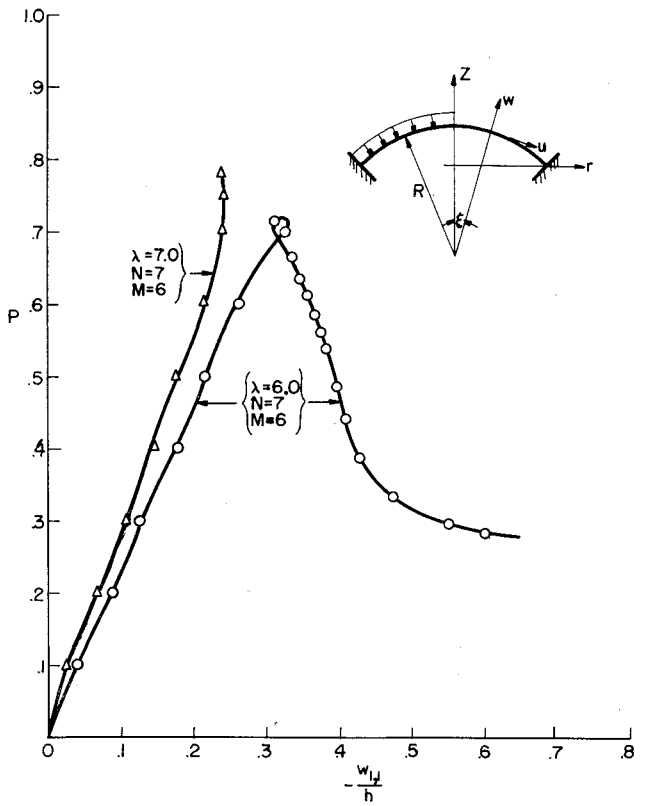

Fig. 7. Load-deflection curves for the half-loaded shell showing the prebuckling and postbuckling ranges for $\lambda = 6$ and only the prebuckling range for $\lambda = 7$ for the deflection point $w_{1,1}$ (near the apex of the shell).

Stability of a Spherical Cap under Asymmetric Loading

In order to indicate the wider range of stability problems that can be studied by means of this method, the problem of the spherical cap subjected to a pressure uniformly distributed over half the surface of the shell is studied. The results are shown in Fig. 7 where the load-deflection curve is computed†† only up to the upper buckling load for $\lambda = 7$ and for the pre- and postbuckling range for $\lambda = 6$ in order to illustrate the possibilities of the method.

6. Conclusions

It is apparent from Figs. 5 and 6 that, in experimental testing or in practice, the existence of imperfections in geometric shapes or other departures from the ideal conditions of the perfect spherical cap under uniform load could cause the failure of the shell before the p_U is reached. It should be noted that the "lower buckling pressures" as computed in Ref. 3 which were based on an axisymmetric theory correspond to the pressure at which the shell "snaps back" from the stable symmetric postbuckled shape to the prebuckled shape. The p_L computed in this paper are not "snap back" loads in the sense of Ref. 3 but represent the lowest point on an asymmetric postbuckling load deflection curve which in the presence of initial imperfections could be a load near which a buckling mechanism involving asymmetric shapes could occur.

Thus the p_L load becomes an important index of the buckling strength of shells fabricated under ordinary standards, and the experimental results shown in Fig. 1 appear to substantiate this assertion. The actual buckling loads are scattered all the way from the neighborhood of p_L (shown by crosses) to p_U (curve C) with the carefully conducted experiments of Ref. 8‡‡ almost reaching the upper load.

The results of this work appear to give the first systematically computed asymmetric postbuckling stress and deformation states available in the literature. Previous solutions of the trial-mode type have involved too few parameters to be reliable and were incapable of direct extension to increase the accuracy. The present solution method is only limited by the users decision on the number of solution points to take.

References

[1] Budiansky, B., "Buckling of clamped shallow spherical shells," *IUTAM Symposium on the Theory of Thin Elastic Shells* (Delft, The Netherlands, 1959), pp. 64–94.

[2] Weinitschke, H. J., "On the stability problem of shallow spherical shells," J. Math. Phys. **38**, 209–231 (1960).

[3] Thurston, G. A., "A numerical solution of the non-linear equations for axisymmetric bending of shallow spherical shells," J. Appl. Mech. **28**, 557–568 (1961).

[4] Archer, R. R., "On the numerical solution of the non-linear equations for shells of revolutions," J. Math. Phys. **41**, 165–178 (1962).

[5] Weinitschke, H. J., "Asymmetric buckling of clamped shallow spherical shells," NASA TN D-1510, pp. 481–490 (1962).

[6] Huang, N. C., "Unsymmetrical buckling of thin shallow spherical shells," TR 15, Div. of Engineering, Harvard Univ., Cambridge, Mass. (1963); also a part of this report was published as "Unsymmetrical buckling of thin shallow spherical shells," AIAA J. **1**, 945 (1963).

[7] Archer, R. R. and Famili, J., "On the vibration and stability of finitely deformed shallow spherical shells," J. Appl. Mech. (to be published); also American Society of Mechanical Engineers Paper 64-WA/APMII.

[8] Krenzke, M. A. and Kiernan, T. J., "Elastic stability of near-perfect shallow spherical shells," AIAA J. **1**, 2855–2857 (1963).

[9] Marguerre, K., "Zur Theorie der Gekrummten Platte grosser Formanderung," Proceedings Fifth International Congress of Applied Mechanics, pp. 93–101 (1938).

[10] Varga, R. S., *Matrix Iterative Analysis* (Prentice-Hall, Inc., Englewood Cliffs, N. J., 1962).

[11] Famili, J., "On the vibration, buckling and postbuckling behavior of shells of revolution under symmetrical and unsymmetrical load," Ph.D. Thesis, Case Institute of Technology (1964).

[12] Kaplan, A. and Fung, Y. C., "A non linear theory of bending and buckling of thin elastic shallow spherical shells," NACA TN 3212 (1954).

[13] Parmerter, R. R., "The buckling of clamped shallow spherical shells under uniform pressure," Air Force Office of Scientific Research 5362, California Institute of Technology p. 87 (November 1963).

†† See Ref. 11 for numerical details of the results in Figs. 5–7.

‡‡ Experimental results reported in Ref. 13 were brought to the author's attention by a referee. These results are scattered both above and below the Huang loads with a maximum discrepancy of about 15% over the range $\lambda = 5$ to 20.